Estimation of Soil Respiration: Improved Techniques for Measurement of Soil Gas

J. M. Blonquist Jr.*[1], S.B. Jones, and B. Bugbee *

Abstract

Respiration can be measured either as an increase in CO_2 or as a decrease in O_2. Because CO_2 can be accurately measured by infrared absorption, CO_2 has been widely used for measurements of soil respiration. However, CO_2 is 30 times more soluble in water than O_2 so the sensitivity of gas phase CO_2 to temperature is 30 times greater than for O_2. This means that measured fluxes of CO_2 from soils can be the result of non-metabolic changes in CO_2 in the gas phase of soil. These considerations are particularly significant when using the gradient flux method of measuring soil respiration because continuous measurement of either CO_2 or O_2 in soil gas is required. We calculated the effects of temperature, barometric pressure, pH, and humidity on CO_2 and O_2 concentrations in soil gas. The effect of temperature on gaseous CO_2 is complex at higher pH values because CO_2 gas is also in equilibrium with bicarbonate in the soil solution. At 25 °C and 0.1 % CO_2 (1000 ppm), our calculations indicate that CO_2 should increase by 0.0015 % CO_2 per °C (15 ppm per °C), and the effect of temperature on O_2 is negligible. Measurements in autoclaved sand (using an infrared sensor for CO_2 and galvanic-cell O_2 sensors that can resolve 0.001 % O_2 (10 ppm)) confirmed these results. The increased sensitivity of infra-red measurement of CO_2 is largely offset by the increased temperature correction for non-

* J.M. Blonquist Jr. of Apogee Instruments, Inc.

* B. Bugbee of Utah State University

metabolic effects of CO_2. Measurement of O_2 should be used to supplement CO_2-based methods of soil respiration.

Introduction

Soil respiration is the sum of root respiration and the decomposition of soil organic matter, plant litter, and root exudates by soil micro-organisms. Soil respiration represents a significant source of carbon flux to the atmosphere and thus is a major component in the global carbon cycle. The understanding of ecosystem carbon cycling responses to global climate change hinges on accurate measurements of soil respiration. Increasingly, measurements of soil respiration rates are included as inputs to global carbon cycling models used to predict global warming effects on soil carbon storage.

Diffusion along concentration gradients is the primary mechanism for gaseous transport in soils, and from soil to the atmosphere, and is described by Fick's Law:

$$J = D_S \frac{dC}{dz} \tag{1}$$

where J is gas flux [mol m^{-2} s^{-1}], D_S is the soil gas diffusion coefficient [m^2 s^{-1}], which is dependent on soil porosity and water content, C is gas concentration [mol m^{-3}], z is soil depth [m], and dC / dz is the concentration gradient driving gas flux. Measurement of the gas concentration profile in soil allows for the estimation of gas flux using discrete differences in concentration and depth, i.e. $dC = \Delta C$ and $dz = \Delta z$ in Eq. (1). Measurement of gas flux in this manner is called the gradient flux method (Tang et al., 2003; Jassal et al., 2005; Turcu et al.,

2005), and it can be used to measure soil surface CO_2 flux, as is done with the commonly used chamber techniques (Rochette and Hutchinson, 2005).

Measurements of CO_2 flux from the soil surface are used as a means of estimating soil respiration rates (Rochette and Hutchinson, 2005). Soil surface CO_2 flux is an indirect measurement of soil respiration rate and it relies on the assumptions that the CO_2 flux is at steady-state and that all CO_2 flux is a result of respiration. Both assumptions can be valid over a short period of time, but soil respiration rate is highly variable. Substrate quality, quantity, and availability; micro-organism population dynamics; temperature, moisture, oxygen concentration, and pH all affect decomposition by soil microbes. Root biomass and the transfer of photosynthate from the leaves to the roots affect root respiration.

In addition to effects from soil respiration, the concentration of CO_2 in the soil atmosphere, and thus the flux to the surface, varies with temperature, water content, and pH because physical and chemical phenomena, such as CO_2 solubility and carbonate equilibria, can consume or produce CO_2. Parsons et al. (2004) measured physically-driven CO_2 fluxes in dry valley ecosystems in Antarctica. Negative CO_2 flux was observed with decreasing soil temperature and positive CO_2 flux was observed with decreasing soil temperature. Parsons et al. (2004) hypothesized that the abiotic factors causing the CO_2 flux were changes in pressure and volume of gases, changes in CO_2 solubility in the soil water, surface adhesion of CO_2 to soil minerals, and pH-driven CO_2 dissolution chemistry. However, the magnitude of the flux caused by each separate effect was not determined. Pressure gradients within soil are a negligible means of gas flux in most soils (Hillel, 1998) and can be ignored. However, the other factors may contribute significantly to soil surface CO_2 flux and must be accounted for in order to accurately estimate soil respiration rates.

Measurement of O_2 flux from the soil surface as a means of estimating soil respiration has the potential to supplement and improve CO_2 flux-based estimates of respiration. There are less abiotic factors to account for in O_2 flux measurement because soil surface O_2 flux is not subject to pH-driven dissolution chemistry, and O_2 is much less soluble in water compared to CO_2 (Gevantman, 2005). Additionally, the two gases can be measured in conjunction to provide a better estimate of soil respiration because of the one to one relationship of the gases in the respiratory process, one mole of O_2 consumed equals one mole of CO_2 evolved. Additionally, the two gases measured in conjunction yields the respiratory quotient, CO_2 produced / O_2 consumed. The purpose of this study was to demonstrate all the necessary corrections to yield accurate measurements of soil O_2 and CO_2 concentration and to model measured effects of CO_2 solubility in water on O_2 and CO_2 measurements.

Theoretical Considerations

Absolute and Relative Gas Concentration

Gas concentration is described in two ways, absolute or relative concentration (Table 1). The ideal gas law yields absolute gas concentration [mol m^{-3}]:

$$PV = nRT \tag{2}$$

where P is pressure [Pa], V is volume [m^3], n is gas quantity [mol], T is temperature [K], R is the ideal gas constant (8.314 J mol^{-1} K^{-1}), and rearranging Eq. (1) to solve for n / V [mol m^{-3}] yields absolute gas concentration (Table 1). However, the simplest and most common way to report the

concentration of a specific gas in a mixture is by expressing it relative to the other gases in the mixture, as a fraction or percentage (Table 1). For example, the amount of oxygen (O_2) in the atmosphere, assuming there is no water vapor in the atmosphere, is 0.2095 kPa O_2 per kPa air or 20.95 % O_2. Gas sensors respond to absolute gas concentration but are generally calibrated to yield relative gas concentration. As pressure and temperature fluctuate, the absolute gas concentration, and thus gas sensor output, fluctuates. If these effects are not accounted for, it produces an apparent change in the relative gas concentration.

The absolute gas concentration determines the rate of most biological and chemical processes, but the relative gas concentration is typically reported. This is analogous to discussing relative humidity when absolute humidity is what determines evaporation rates. For example, the dry atmospheric concentration of O_2 has remained constant for several hundred years at 20.9476 %. The percentage is the same at sea level or any elevation. However, the absolute O_2 concentration does not remain constant. An O_2 tank is required to climb Mount Everest, even though the relative O_2 concentration is still 20.95 % (Fig. 1A). Absolute and relative gas concentration measurements can be expressed using several different units (Table 1).

Effect of Barometric Pressure on Gas Concentration

The ideal gas law (Eq. (2)) states that at constant temperature, absolute gas concentration increases by 0.987 % at sea level for every 1 kPa increase in pressure (1 kPa / 101.325 kPa = 0.00987). If not accounted for in a relative gas measurement, this leads to apparent gas concentration changes with pressure. For example, a 1 kPa pressure increase from 101.325 kPa results in an apparent increase of 0.207 % O_2 (0.987 % * 0.2095 = 0.207 %) and a relative O_2 concentration of 21.157 %. Due to lower barometric pressure at higher elevations (Fig. 1A), the

percentage increase in absolute gas concentration per kPa increases with elevation. For example, at an elevation of 1358 m (elevation of Logan, UT), the barometric pressure is approximately 86 kPa and the absolute gas concentration increases by 1.16 % for every 1 kPa increase in pressure (1 kPa / 86 kPa = 0.0116).

To calculate the effect of pressure on relative gas measurements, approximate barometric pressure (*BP*) [kPa] can be calculated according to (reference):

$$BP = 101.325 \left(\frac{288 - 0.0065E}{288} \right)^{5.25328} \tag{3}$$

where E is elevation [m]. Due to the apparent change in relative gas measurements with barometric pressure changes, a correction should be applied to all sensors that are calibrated to read relative gas concentration. The equation to correct relative O_2 measurements for barometric pressure at any elevation is:

$$O_2 = O_{2M} \left[1 - \left(\frac{BP_M - BP_C}{BP_C} \right) \right] \tag{4}$$

where O_{2M} is measured O_2 concentration [%] (the apparent O_2 concentration), BP_M is barometric pressure [kPa] at the time of the measurement, and BP_C is barometric pressure [kPa] at the time of sensor calibration. The apparent effect of barometric pressure on relative O_2 measurements, based on calculations from Eq. (4), are plotted for a 1358 m elevation (Fig. 1B) to show the significance of measuring and correcting for barometric pressure.

Effect of Temperature on Gas Concentration

The ideal gas law (Eq. (2)) states that at constant pressure, absolute gas concentration decreases by 0.341 % for a 1 °C increase in temperature from 20 °C (1 K / 293 K = 0.00341). If not accounted for in a relative gas measurement, this leads to apparent gas concentration changes with temperature. For example, a 1 °C temperature increase from 20 °C results in an apparent decrease of 0.071 % O_2 (0.341 % * 0.2095 = 0.071 %) and a relative O_2 concentration of 20.879 %. To obtain accurate relative gas measurements a correction should be applied to compensate for temperature effects. The equation to correct O_2 measurements in air for temperature effects is:

$$O_2 = O_{2M}\left[1 + \left(\frac{T_M - T_C}{T_C}\right)\right] \tag{5}$$

where O_{2M} is as given above, T_M is the air temperature [K] at the time of the measurement, and T_C is the air temperature [K] at calibration. The effects of temperature on relative O_2 measurements, based on calculations from Eq. (5) are plotted (Fig. 2) to show the significance of measuring and correcting for temperature.

Effect of Humidity on Gas Concentration

As the humidity in the atmosphere increases, water vapor molecules displace and dilute other gas molecules, causing the output of a gas sensor to decrease. The effect of water vapor displacement of gas molecules is larger at warmer temperatures because the capacity of air to hold water is greater and there is more water vapor in the air. The water vapor effect on relative gas concentration as a function of relative humidity (*RH*) at a constant temperature is a linear

decrease with increasing *RH*, as shown for O_2 (Fig. 3). Conversely, the effect as a function of temperature at constant *RH* is a curvilinear decrease with increasing temperature (Fig. 3), essentially the inverse of the slope of the vapor pressure curves from the pyschrometric chart. Even though water vapor molecules dilute and diplace gas molecules, and thus cause an actual and not an apparent decrease in relative gas concentration, humidity effects are accounted for to yield relative gas concentrations for a dry atmosphere. The equation to correct relative O_2 measurements for humidity effects is:

$$O_2 = O_{2M}\left[1+\left(\frac{e_{AM}-e_{AC}}{BP_C}\right)\right] \tag{6}$$

where O_{2M} and BP_C are as given above, e_{AM} is the vapor pressure [kPa] of the air at the time of measurement, and e_{AC} is the vapor pressure [kPa] of the air at calibration. The vapor pressures in Eq. (6) are calculated from:

$$e_A = e_S\left(\frac{RH}{100}\right) \tag{7}$$

where *RH* is in % and e_S is the saturation vapor pressure [kPa] of the air calculated from air temperature (T_A) [°C] (Buck, 1981):

$$e_S = 0.61121\exp\left(\frac{17.502T_A}{240.97+T_A}\right). \tag{8}$$

In soil environments *RH* is generally always 100 %, unless the soil is extremely dry. Thus, the water vapor effect can be accounted for as a function of temperature by correcting gas measurements based on the shape of the curve for 100 % *RH.*

Effect of Gas Solubility in Water

Gas solubility is a function of temperature, with changes in temperature causing gas to go into or come out of solution. For example, the solubility of CO_2 and O_2 in water as a function of temperature show both gases are more soluble at lower temperatures (Fig. 4; solubility data are from Gevantman (2005)). Similar to water vapor molecules diluting and displacing gas molecules as humidity increases, molecules of a specific gas coming out of solution can also dilute and displace gas molecules. For example, using CO_2 solubility data from Gevantman (2005), the effects of CO_2 solubility at two different initial soil CO_2 concentrations (0.1 and 1.0 %; common for many soils) on O_2 and CO_2 measurements were calculated as a function of temperature (Fig. 5) according to:

$$CO_2 = 100 \cdot \frac{\left[\left(\Delta dissolvedCO_2\right)\left(\frac{1}{M_{H_2O}}\right)\left(\rho_{H_2O}\right)\left(V_{H_2O}\right)\right] + \left[\left(\frac{CO_{2-initial}}{100}\right)\left(\rho_{mol-air}\right)\left(V_{air}\right)\right]}{\left[\left(\Delta dissolvedCO_2\right)\left(\frac{1}{M_{H_2O}}\right)\left(\rho_{H_2O}\right)\left(V_{H_2O}\right)\right] + \left[\left(\rho_{mol-air}\right)\left(V_{air}\right)\right]} \quad (10)$$

where CO_2 is relative concentration [%], $\Delta dissolvedCO_2$ is the change in CO_2 dissolved in water [mmol CO_2 mol H_2O^{-1}], which is temperature dependent, M_{H2O} is the molar mass of water (18 g mol^{-1}), ρ_{H2O} is the density of water (1000 g L^{-1}), V_{H2O} is the volume of water [L], $CO_{2\text{-}initial}$ is the

initial relative concentration [%], $\rho_{mol\text{-}air}$ is the molar density of air (41.6 mmol L^{-1} at 101.325 kPa and 20 °C), and V_{air} is the volume of air [L].

Materials and Methods

Sensor Description

The oxygen sensors (Apogee Instruments models O2S-D-S-TM, soil sensor; and O2S-D-FR-TM, fast response sensor) used for all measurements are galvanic cell sensors with a lead anode, gold cathode, acid electrolyte, and Teflon membrane. The current flow between the two electrodes is linearly proportional to the absolute amount of O_2 in the environment being measured. An internal bridge resistor is used to produce a voltage output rather than a direct current output. Galvanic cell sensors consume a small amount of gas in order to produce the current flow between the electrodes and subsequent voltage output. The O_2 consumption from the sensors used was measured to be 2.1 μmol per day at 20.95 % O_2 and at an average temperature of 20 °C in a small sealed chamber. All sensors were equipped with an internal thermistor for reference temperature measurement.

The response time of the soil sensor is 60 seconds versus 14 seconds for the fast-response sensor. The output signal for the soil sensor is approximately 58.0 mV under typical atmospheric conditions (20.95 % O_2 and 101.325 kPa) and the average signal decrease is reported as 1.0 mV per year (< 2.0 % per year). The output signal for the fast-response sensor is approximately 12.8 mV under standard atmospheric conditions and the signal decrease is reported as 0.8 mV per year (< 6.0 % per year up to 5 years). The manufacturer reports the output to be linear as a function of O_2 concentration. A single-point calibration was used to derive a calibration factor

used to convert mV output from the sensor to % O_2. Before any measurements were taken the sensors were calibrated in ambient conditions and over water in a small, sealed container. The ambient calibration was used in the dry air and dry sand experiments and the calibration over water was used in the wet sand experiments, all described below. The purpose of the calibration over water is to account for a small effect of water vapor on sensor electronics/electrolyte, as reported by the manufacturer.

The sensors come equipped with an internal thernistor and a small resistance heater located behind the membrane inside the sensor. The heaters are designed to warm the sensor to a temperature slightly above ambient in order to keep condensation from occurring on the membrane under conditions where the *RH* is 100 %. For all measurements, the heaters were connected in order to account for the effect of the heater on the temperature response of the sensors. The onboard thermistors were used to measure the sensor temperature. Also, throughout the course of the dry air, dry sand, and wet sand measurements (described below), barometric pressure was measured with a transducer (OMEGA model EWS-BP-A Barometric Pressure Transducer) so the described barometric pressure correction could be applied.

Measurements in Dry Air

Oxygen measurements with three replicate soil sensors and three replicate fast-response sensors were made in air in a temperature-controlled, enclosed chamber over a temperature range of 0 to 50 °C, at 5 °C intervals. The temperature was cycled from approximately 0 to 50 °C, then back to 0 from 50 °C. At each measurement step, the temperature was held constant for two hours to allow the sensors to equilibrate. Dry air (dessicated to < 2 % *RH* as measured with Vaisala model HMP-45) was pumped into the enclosure containing the sensors to minimize

water vapor dilution effects. A datalogger (Campbell Scientific model CR10T) and multiplexer (Campbell Scientific model AM25T) were used to make all measurements at two-second intervals. The datalogger was programmed to calculate and record five-minute averages for each sensor (i.e. average of 150 measurements). The last five-minute average for each given temperature step, before the temperature increased or decreased to the next temperature step, was taken as the mV measurement value (proportional to O_2 concentration) for the given step.

Measurements in Dry Sand

Following the measurements in dry air the O_2 sensors were buried in a large container of sand (Fig. 6). The container measured approximately 0.02 m^3 (20 liters) in volume and the sand was oven dried at 105 °C for 24 hours before the sensors were buried in it. After drying, the water content was measured gravimetrically to be less than 0.01 $m^3\ m^{-3}$. The dry mass of the sand was measured to be approximately 32 kg, giving the sand a bulk density of 1600 kg m^{-3}. Assuming the sand solid density was 2650 kg m^{-3}, the porosity was calculated as 0.4 $m^3\ m^{-3}$. Eight 60-W resistance heaters were buried in the sand along with the sensors. The heaters were used to cycle the temperature up and down. The temperature was cycled up and down twice over the course of a sixteen day period during which O_2 measurements were made every two seconds and averaged over a five-minute period. Three type-E thermocouples were also buried in the sand alongside the O_2 sensors in order to measure the sand temperature (thermocouples were connected to the AM25T multiplexer). One CO_2 sensor (Vaisala model GMD20) was buried in the sand alongside the O_2 sensors. The *RH* of the air in the sand was measured periodically with an *RH* meter (Vaisala model HMP-45) and varied between 10 and 30 % over the sixteen day period.

Measurements in Wet Sand

Following the measurements in dry sand, approximately 0.004 m^3 (4 liters) of water was added to the sand to increase the water content to approximately 0.2 m^3 m^{-3}. After the water was added approximately half of the pore space (porosity was approximately 0.4 m^3 m^{-3}) contained water and half contained air. The temperature was cycled up and down twice over the course of a twenty-six day period and measurements were made every two seconds and averaged over a five-minute period, as in the dry sand. The same datalogger and multiplexer set-up described for the dry air measurements was used for the dry and wet sand measurements.

Results and Discussion

Response to Temperature in Dry Air

In practice, Eq. (5) may not accurately correct for temperature effects because in addition to the ideal gas law temperature effect, the sensor electronics are sensitive to temperature. The combination of these two effects was determined from the dry air data by plotting pressure-corrected apparent O_2 concentration versus the sensor temperature (Fig. 7) measured with the internal thermistor. Neither of the sensor models follows the ideal gas law temperature response, where difference between the theoretical and measured responses is due to a temperature effect on the sensor electronics. An empirical temperature correction derived from the measured data must be applied to account for the combination of the ideal gas law and sensor electronic responses:

$$O_2 = O_{2M} + C_3 T^3 + C_2 T^2 + C_1 T^1 + C_0 \tag{11}$$

where T is the measured sensor temperature [°C], the polynomial coefficients C_3, C_2 and C_1 are listed in Fig. 7 for both the soil and fast-response sensors, and C_0 is the offset coefficient calculated from the temperature at calibration, T_C [°C]:

$$C_0 = -\left(C_3 T_C{}^3 + C_2 T_C{}^2 + C_1 T_C{}^1\right). \tag{12}$$

The offset coefficient scales the temperature response curves in Fig. (9) up or down dependent on the temperature at calibration.

Pressure Correction

The uncorrected measurements in dry and wet sand show large deviations from 20.95 % O_2 (Figs. 8A and 8B) even though the sand used herein was autoclaved and the O_2 concentration should have remained constant at ambient concentration. Equation (4) was applied to the dry and wet sand measurements to correct for barometric pressure effects (Figs. 8C and 8D). During the dry sand measurements the pressure ranged from 85.7 – 87.0 kPa, causing a maximum apparent O_2 change of approximately 0.3 %. The pressure range during the wet sand measurements was 84.8 – 87.1 kPa, yielding a maximum apparent O_2 change of 0.6 %. Relative to the large fluctuations caused by temperature, the pressure effect is small. Going from A and B to C and D in Fig. 8, it is somewhat difficult to see the improvement in the data resulting from the barometric pressure correction, but the pressure correction does improve the uncorrected measurements (Figs. 8C and 8D). For example, the temperature was relatively constant from day

0 – day 6 during the wet sand measurements. During this time frame, the improvement of the pressure correction can be seen (Figs. 8A and 8B compared to Figs. 8C and 8B).

Temperature Correction

Applying Eqs. (11) and (12) to the pressure-corrected data yields improved measurements in both the dry sand and wet sand (Figs. 8E and 8F compared to Figs. 8C and 8D). The dry sand measurements were averaged over the course of the whole experiment yielding average % O_2 values of 20.95 % ± 0.14 % and 20.95 % ± 0.19 % (two standard deviations) for the soil sensor and fast-response sensor, respectively, or variation of less than 1 % from the mean value.

The temperature effect on the sensor electronics varies from sensor to sensor (see error bars in Fig. 7), thus the coefficients derived herein (the average of the three replicate sensors for each sensor type used in the experiments) may not yield the most accurate temperature correction for all sensors of the same model.

Humidity Response

The humidity correction was not applied to the dry sand measurements because humidity was not continuously measured throughout the course of the experiment. Periodic measurements showed the *RH* of the sand varied from 10 to 30 % during the dry measurements. When the temperature is warmer the air holds more water vapor and the O_2 concentration decreases. The O_2 measurements for the periods when the heaters were on show this trend, they were slightly lower when the heaters are on, creating a small cycle in % O_2 from un-heated to heated periods (Fig. 8E).

The relative humidity was also not continuously measured during the wet sand measurements, but the humidity correction (Eqs. (6) – (8)) was applied to the wet sand measurements (Fig. 7G) assuming the relative humidity was always 100 %, a valid assumption for wet soils. The wet sand measurements were averaged over the course of the whole experiment yielding average % O_2 values of 20.96 % ± 0.14 % and 20.97 % ± 0.17 % (two standard deviations) for the soil sensor and fast-response sensor, respectively, or variation of less than 1 % from the mean value.

CO_2 and O_2 Solubility Effects

The solubility of CO_2 is much greater than O_2, with the ratio of CO_2 to O_2 solubility in water ranging from 34 to 21 from 0 to 50 °C (Fig. 4). Because O_2 solubility is much smaller relative to CO_2 solubility, and because the background concentration of O_2 is generally much greater (approximately two orders of magnitude) than CO_2, O_2 solubility effects on O_2 and CO_2 measurements are negligible and can generally be ignored. Assuming sensor calibrations at 20 °C, the change in O_2 and CO_2 concentration as CO_2 goes into or comes out of solution across a temperature range of 0 to 50 °C shows a minimal effect on O_2 concentration, but has a large effect on CO_2 concentration (Fig. 5). At a background CO_2 concentration of 1.0 %, a 5 °C decrease from 20 °C yields an O_2 concentration of 20.98 % and a 5 °C increase from 20 °C yields an O_2 concentration of 20.92 % (Fig. 5), or a change of 0.007 % O_2 per °C increase. At a background CO_2 concentration of 1.0 %, a 5 °C decrease from 20 °C yields a CO_2 concentration of 0.85 % and a 5 °C increase from 20 °C yields an O_2 concentration of 1.12 % (Fig. 5), or a change of approximately 0.027 % CO_2 per °C increase. These calculations assume the soil pore

space contains 50 % air and 50 % water (i.e. in Eq. (10) $V_{H20} = V_{air}$). The solubility effect would be greater if the soil contained more water and smaller if the soil contained less water.

Using the theoretical concentration data from Fig. 5, and assuming fixed concentrations at the soil surface, the change in the driving gradient was calculated. The effect of CO_2 solubility on O_2 concentration gradient ($\partial C / \partial z$ from Eq. (1)) is negligible (Fig. 9A) and can be ignored when calculating an O_2 concentration gradient, but the effect on CO_2 concentration is significant (Fig. 9B) and must be accounted for, otherwise temperature changes causing CO_2 to go into or come out of solution will be interpreted as changes in respiration because the gradient driving CO_2 flux changes.

The CO_2 concentration measurements from the dry ($\theta_v < 0.01$ m^3 m^{-3}) and wet ($\theta_v = 0.2$ m^3 m^{-3}) sand confirm the model (Eq. (10)) showing the effects of CO_2 solubility in Fig 5. In dry sand the difference in CO_2 with increasing temperature was negligible, but the CO_2 concentration increases with temperature in the wet sand (Fig. 10A). The CO_2 measurements in dry sand are not affected by changing temperature because there is a minimal solubility effect under dry conditions. The slope was 0.0000629 % CO_2 $°C^{-1}$, a change of only 0.13 % per °C from the 0.0492 % CO_2 concentration at 25 °C. In wet sand the measured CO_2 concentration increased by 0.00144 % CO_2 $°C^{-1}$, which is a change of 1.6 % per °C from the 0.0911 % CO_2 concentration at 25 °C. This measured change compared very well to the predicted CO_2 change (Eq. (10)) based on CO_2 solubility effects (Fig. 10A). The model slope was 0.00146 % CO_2 $°C^{-1}$. This gives strong evidence that the CO_2 concentration in wet sand increased with increasing temperature because CO_2 solubility decreases with increasing temperature and CO_2 came out of solution.

There was not a detectable effect of CO_2 solubility on the O_2 measurements (Fig. 10B). The reason for the O_2 measurements decreasing with temperature in dry sand is likely due to the

lack of a humidity correction in the dry sand measurements. As explained above, this correction was not applied because humidity was not continuously measured during the dry sand measurements. The slight decrease is due to more water vapor in the air at higher temperatures because the capacity of the air to hold water vapor increases with temperature.

Application to Soil Respiration Estimation

Soil O_2 fluxes provide an estimate of soil respiration that is much less sensitive to temperature because O_2 concentrations are one to two orders of magnitude greater than CO_2 concentrations in soil and O_2 solubility is about 30 times less than CO_2 solubility. Changes in temperature give rise to non-metabolic fluxes of CO_2. If the CO_2 concentrations measured in the wet sand (Fig 10A) as a function of temperature were used to determine CO_2 gradients, the gradient, and thus flux, would increase by approximately 13 % as the temperature increased from 25 to 30 °C. If not accounted for, flux changes due to physical effects are interpreted as changes in respiration. The effect of CO_2 solubility increases as soil water content increases because there is a larger CO_2 source/sink.

Paired O_2 and CO_2 flux measurements in soil have the potential to improve estimation of soil respiration because one mole of O_2 consumed equals one mole of CO_2 evolved. Because O_2 and CO_2 are generally measured in relative terms, multiple corrections are required to account for physical effects that change absolute gas concentration. In order to use gas flux measurements to estimate soil respiration, the necessary corrections to gas concentration measurements must be applied. Barometric pressure, temperature, humidity, and solubility changes must all be accounted for. Humidity and solubility changes are mediated by temperature.

Conclusions

Measurements of CO_2 concentration in wet (θ_v = 0.2 m^3 m^{-3}), autoclaved sand confirmed theoretical predictions of CO_2 concentration change arising from CO_2 solubility as a function of temperature. The temperature effect on CO_2 solubility must be accounted for when using CO_2 flux measurements to estimate soil respiration, otherwise temperature changes producing CO_2 flux changes may be interpreted as soil respiration changes, not CO_2 solubility effects.

Measurements of O_2 are much less sensitive to the CO_2 solubility effect because the concentration of O_2, 20.95 % under ambient conditions, is approximately two orders of magnitude greater than typical CO_2 concentration in the soil. In addition to the negligible effect of CO_2 solubility on relative O_2 concentration, the effects of O_2 solubility are negligible because O_2 is approximately 30 times less soluble than CO_2.

Paired O_2 and CO_2 measurements in soil have the potential to improve characterization of soil respiration. Both measurements require multiple corrections, which account for physical effects that change absolute gas concentrations, in order to yield accurate measurements of relative gas concentration, because O_2 and CO_2 are generally reported in relative terms. The necessary corrections for accurate gas measurement are barometric pressure, temperature, and humidity, and are demonstrated herein. The necessary corrections for accurate CO_2 measurements are the same with the addition of a correction to account for CO_2 solubility effects as a function of temperature.

Acknowledgements

We would like to express thanks to Ray Johnson for help with the graphics.

References

Buck, A. 1981. New equations for computing vapor pressure and enhancement factor. J. Applied Meteorology, 20:1527-1532.

Gevantman, L.H. 2005. Solubility of selected gases in water. In D.R. Lide (editor), Handbook of Chemistry and Physics, 86th Edition pp. 8-80 – 8-83. CRC Press, Boca Raton, FL, USA.

Hillel, D. 1998. Environmental Soil Physics. Academic Press, New York, NY, USA.

Jassal, R., A. Black, M. Novak, K. Morgenstern, Z. Nesic, and D. Gaumont-Guay. 2005. Relationship between soil CO_2 concentrations and forest-floor CO_2 effluxes. Agricultural and Forest Meteorology, 130:176-192.

Parsons, A.N., J.E. Barrett, D.H. Wall, and R.A. Virginia. 2004. Soil carbon dioxide flux in Antarctic dry valley ecosystems. Ecosystems, 7:286-295.

Rochette, P., and G.L. Hutchinson. 2005. Measurement of soil respiration in situ: Chamber Techniques. In J.L. Hatfield and J.M. Baker (editors), Micrometeorology in agricultural systems, pp. 247-286. American Society of Agronomy, Madison, WI, USA.

Tang, J., D.D. Baldocchi, Y. Qi, and L. Xu. 2003. Assessing soil CO_2 efflux using continuous measurements of CO_2 profiles in soils with small solid-state sensors. Agricultural and Forest Meteorology, 118:207-220.

Turcu, V.E., S.B. Jones, and D. Or. 2005. Continuous soil carbon dioxide and oxygen measurements and estimation of gradient-based gaseous flux. Vadose Zone J, 4:1161-1169.

Table 1. Units used to describe absolute and relative gas concentration measurements.

Absolute amount of gas	Relative amount of gas
moles of gas per unit volume (e.g. moles per Liter)	**percent gas in air** (e.g. 20.95 % O_2 in ambient air)
mass of gas per unit volume (e.g. grams per Liter; O_2 has a mass of 32 g per mole and CO_2 has a mass of 44 g per mole)	**mole fraction** (e.g. moles of gas per mole of air; 0.2095 mol O_2 per mole of ambient air; also expressed as 0.2095 kPa O_2 per kPa air)
partial pressure (e.g. kilopascals [kPa])	**parts per million (ppm)** (e.g. 209500 parts O_2 per 1000000 parts ambient air)

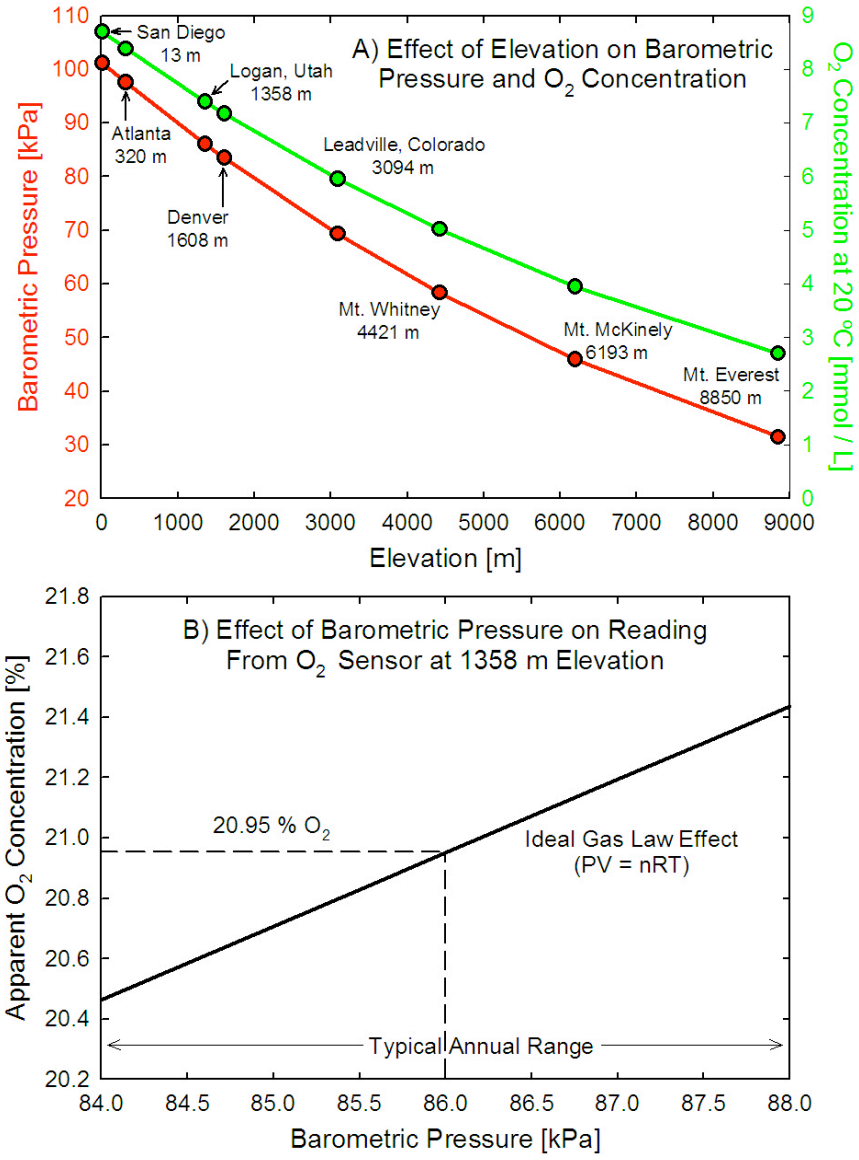

Figure 1: A) Barometric pressure and absolute O_2 concentration [mmol / L] at 20 °C as a function of elevation. Equation (2) was used to calculate barometric pressure. B) The effect of barometric pressure on apparent relative O_2 concentration (i.e. O_2 concentration measured with an O_2 sensor). It is assumed the sensor was calibrated at 86.0 kPa. The solid line shows how the apparent relative O_2 concentration is dependent on barometric pressure.

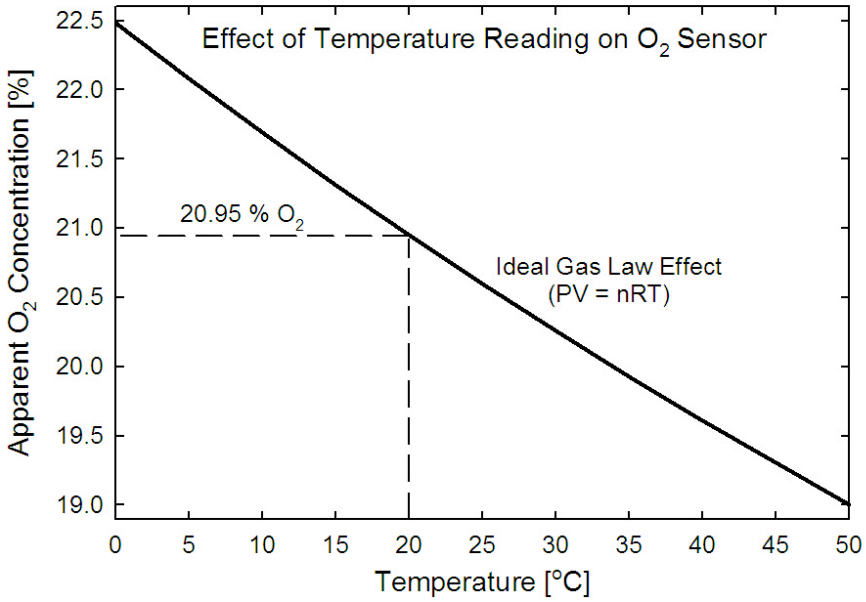

Figure 2: The effect of temperature on apparent relative O_2 concentration (i.e. O_2 concentration measured with an O_2 sensor). It is assumed the sensor was calibrated at 20.0 °C. The solid line shows how the apparent relative O_2 concentration is dependent on temperature.

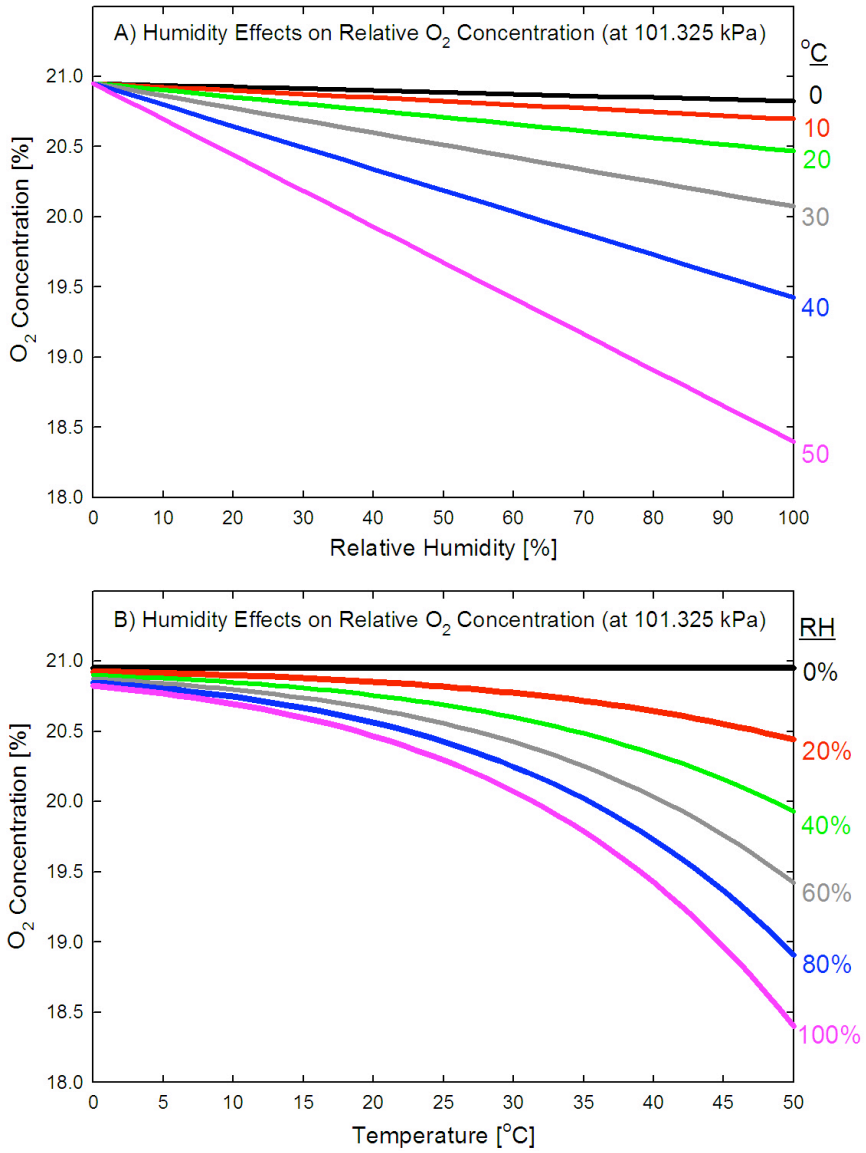

Figure 3: A) Relative humidity (RH) effects on relative O_2 concentration shown as a function of RH at temperatures increments of 10 °C and B) as a function of temperature at RH increments of 20 %. The air in soil is generally always saturated with water vapor unless the soil is very dry, thus only the 100 % RH line applies to soil.

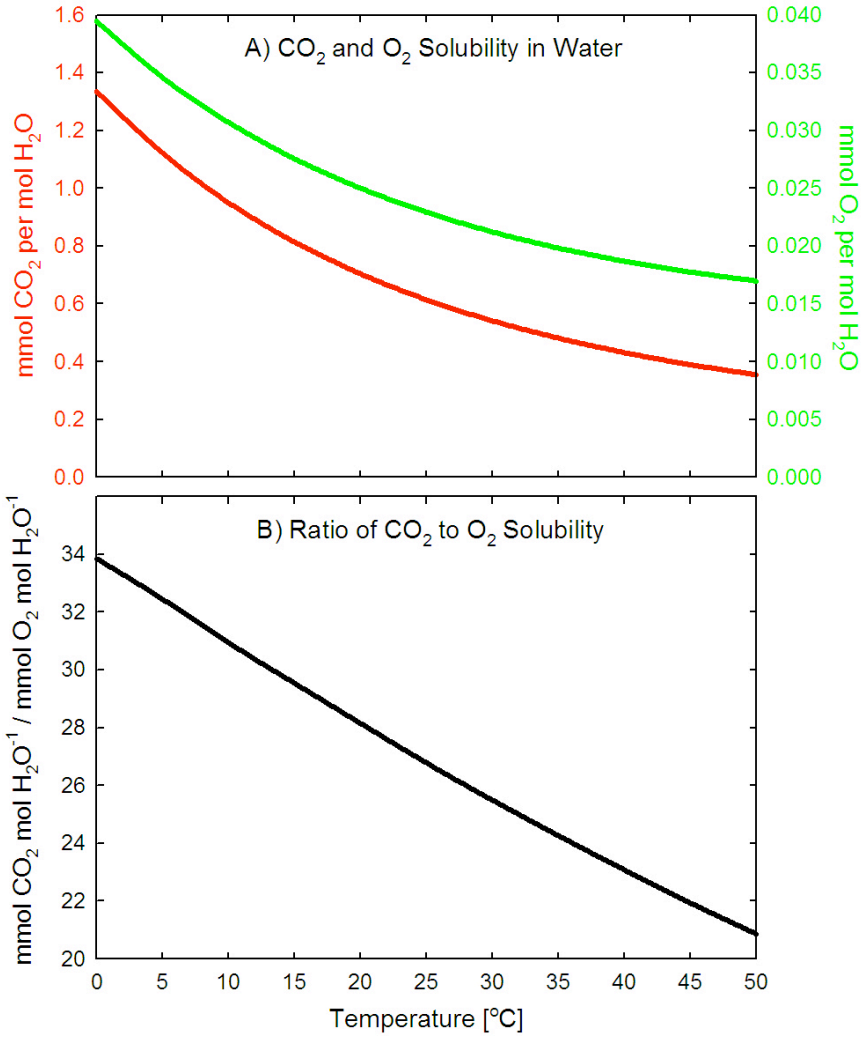

Figure 4: A) Solubility of CO_2 and O_2 in water (data from Gevantman (2005)) and B) the ratio of CO_2 to O_2 solubility as a function of temperature. At colder temperatures CO_2 and O_2 are more soluble than at warmer temperatures, but CO_2 solubility is much greater than O_2 solubility (note the scale differences in A). The solubility of CO_2 ranges from approximately 34 to 21 times that of O_2, and is 28 times greater at 20 °C.

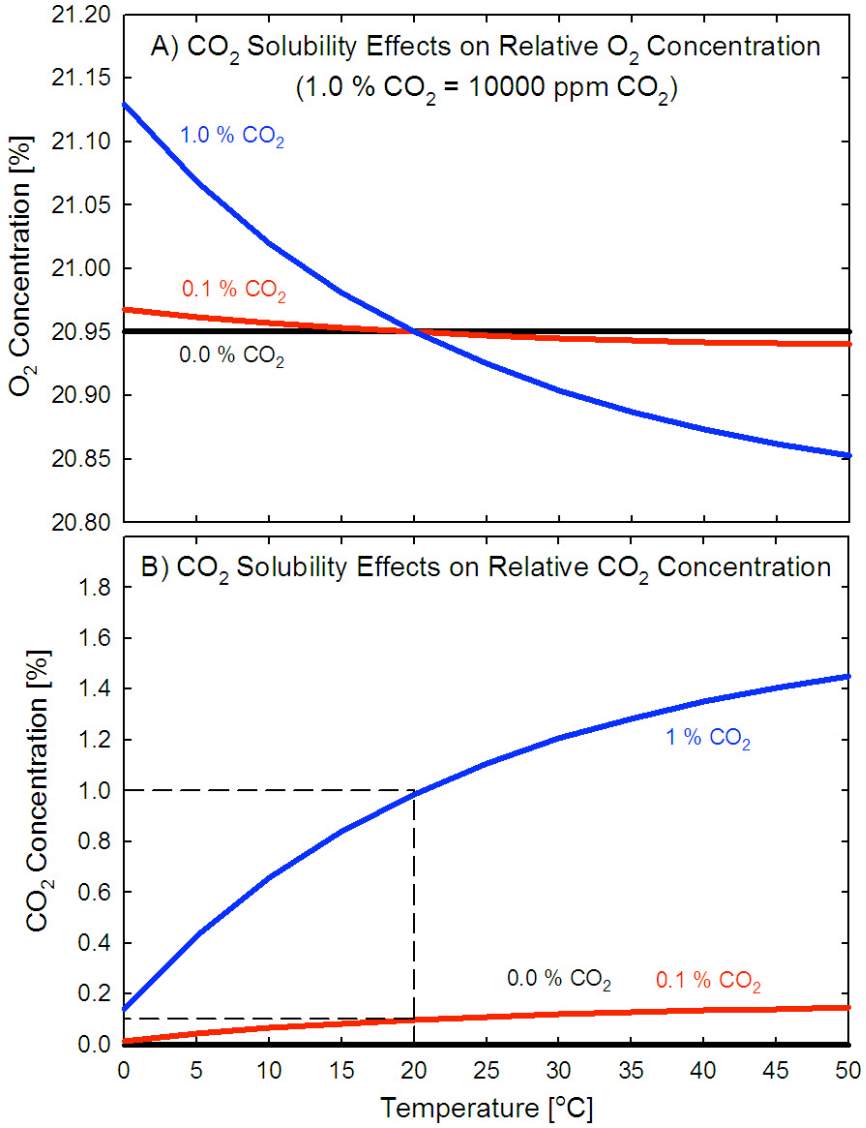

Figure 5: Carbon dioxide (CO_2) solubility effects on relative A) O_2 and B) CO_2 concentration as a function of temperature. The effect for two different background CO_2 concentrations (0.1 and 1.0 %) is shown. At colder temperatures CO_2 is more soluble and at warmer temperatures CO_2 is less soluble. The graphs show the relative change in O_2 and CO_2 concentration as CO_2 goes into or comes out of solution across a temperature range of 0 – 50 °C.

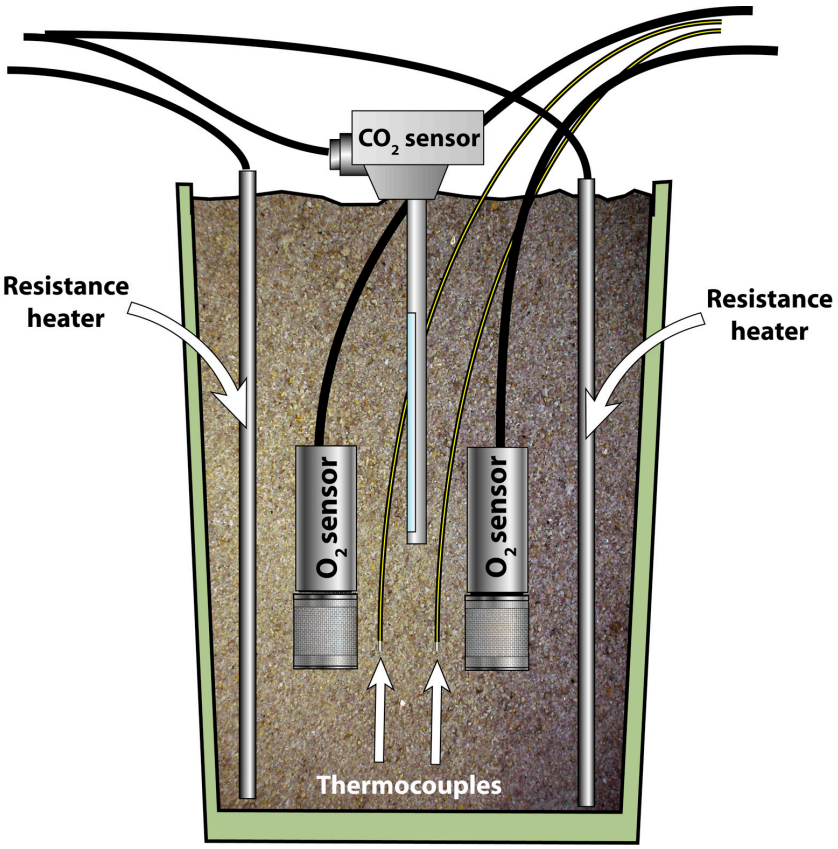

Figure 6: Diagram of the measurements in sand. For clarity in demonstrating the experiment set-up only two O_2 sensors, two resistance heaters, two thermocouples, and one CO2 sensor are shown. In the actual experiment in the sand there were six O_2 sensors (three replicate soil sensors and three replicate fast response sensors), one CO_2 sensor, eight resistance heaters and three thermocouples.

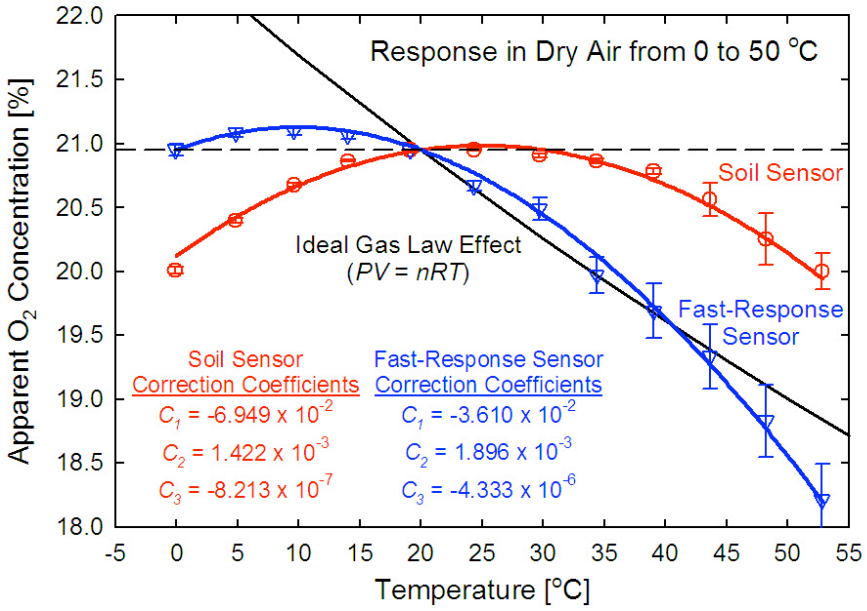

Figure 7: Empirically-measured temperature responses of the soil and fast-response O_2 sensors, with third order polynomials fit to the data points, compared to the theoretical temperature response calculated from the ideal gas law (Eq. (2)). The polynomial coefficients used to correct for the temperature response with Eq. (11) are listed. An offset coefficient (C_0) is not listed because it is be dependent on the temperature at calibration and can be calculated with Eq. (12).

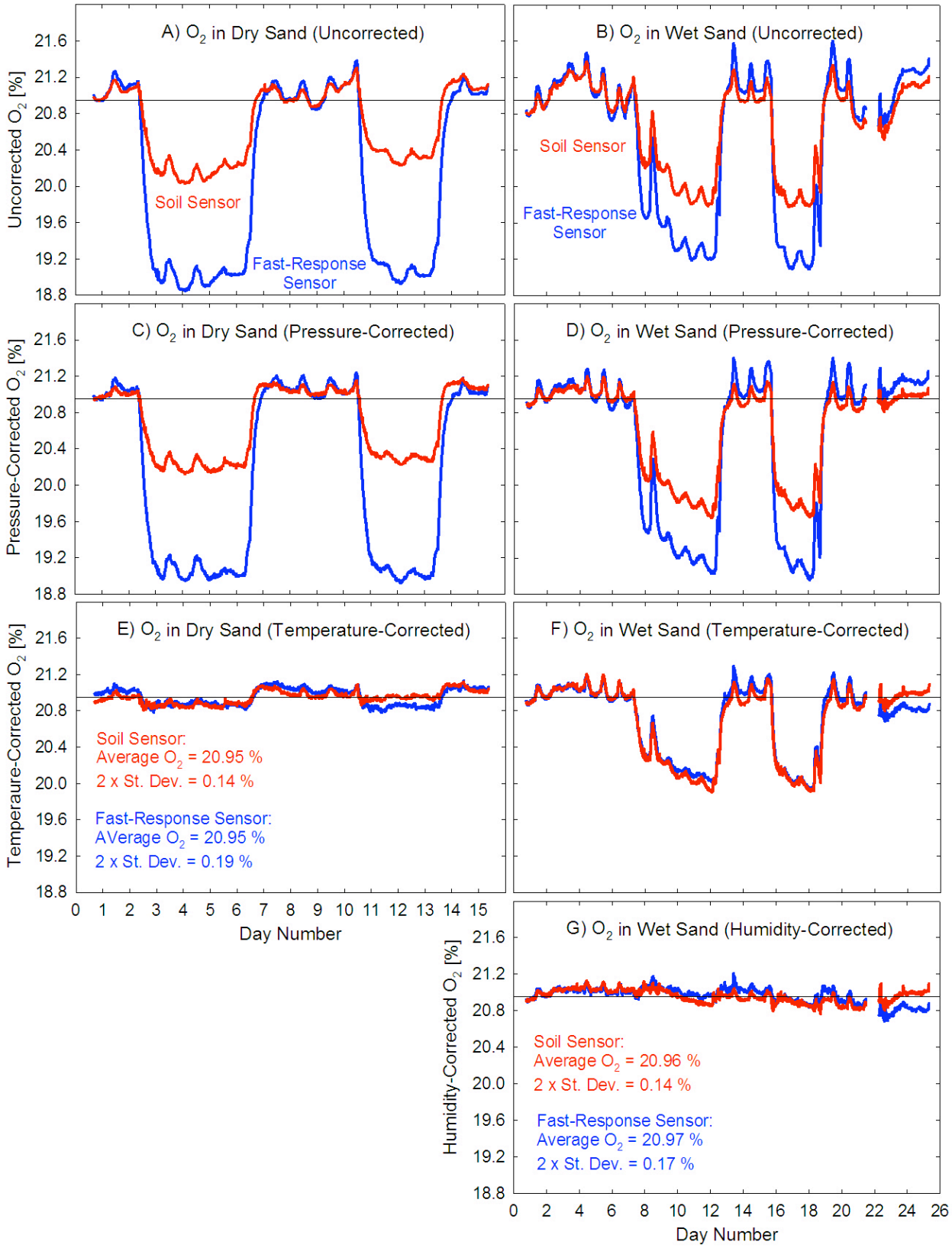
A) O2 in Dry Sand (Uncorrected)
B) O2 in Wet Sand (Uncorrected)
C) O2 in Dry Sand (Pressure-Corrected)
D) O2 in Wet Sand (Pressure-Corrected)
E) O2 in Dry Sand (Temperature-Corrected)
F) O2 in Wet Sand (Temperature-Corrected)
G) O2 in Wet Sand (Humidity-Corrected)
Uncorrected O2 [%]
Pressure-Corrected O2 [%]
Temperaure-Corrected O2 [%]
Humidity-Corrected O2 [%]
Soil Sensor
Fast-Response Sensor
Soil Sensor:
Average O2 = 20.95 %
2 x St. Dev. = 0.14 %
Fast-Response Sensor:
AVerage O2 = 20.95 %
2 x St. Dev. = 0.19 %
Soil Sensor:
Average O2 = 20.96 %
2 x St. Dev. = 0.14 %
Fast-Response Sensor:
Average O2 = 20.97 %
2 x St. Dev. = 0.17 %
Day Number

Figure 8: A) and D) Uncorrected relative O_2 concentration measurements for the soil and fast-response sensors in dry sand and wet sand. C) and D) Data from A and B corrected for barometric pressure effects using Eq. (3). E) and F) Data from C and D corrected for temperature effects using Eq. (11). G) Data from F corrected for humidity effects using Eq. (6) (wet sand only). The described correction for CO_2 solubility effects as a function of temperature was not applied because of the negligible effect on O_2 concentration (Fig. 3).

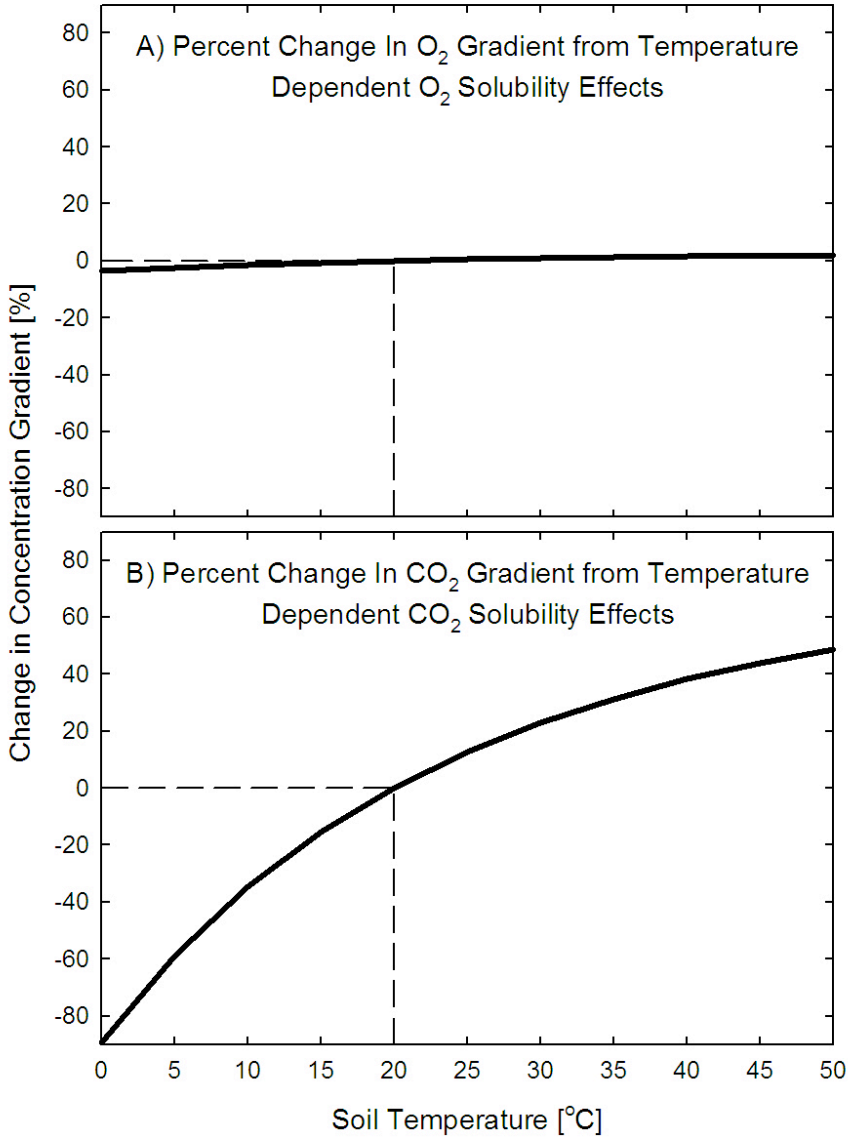

Figure 9: Percent change in the A) O_2 and B) CO_2 gradient as a result of CO_2 solubility changing with temperature. Changes in the O_2 gradient due to CO_2 solubility can generally be ignored, but changes the CO_2 gradient must be accounted for, otherwise a change in CO_2 flux is interpreted as a change in soil respiration rather than a physical effect.

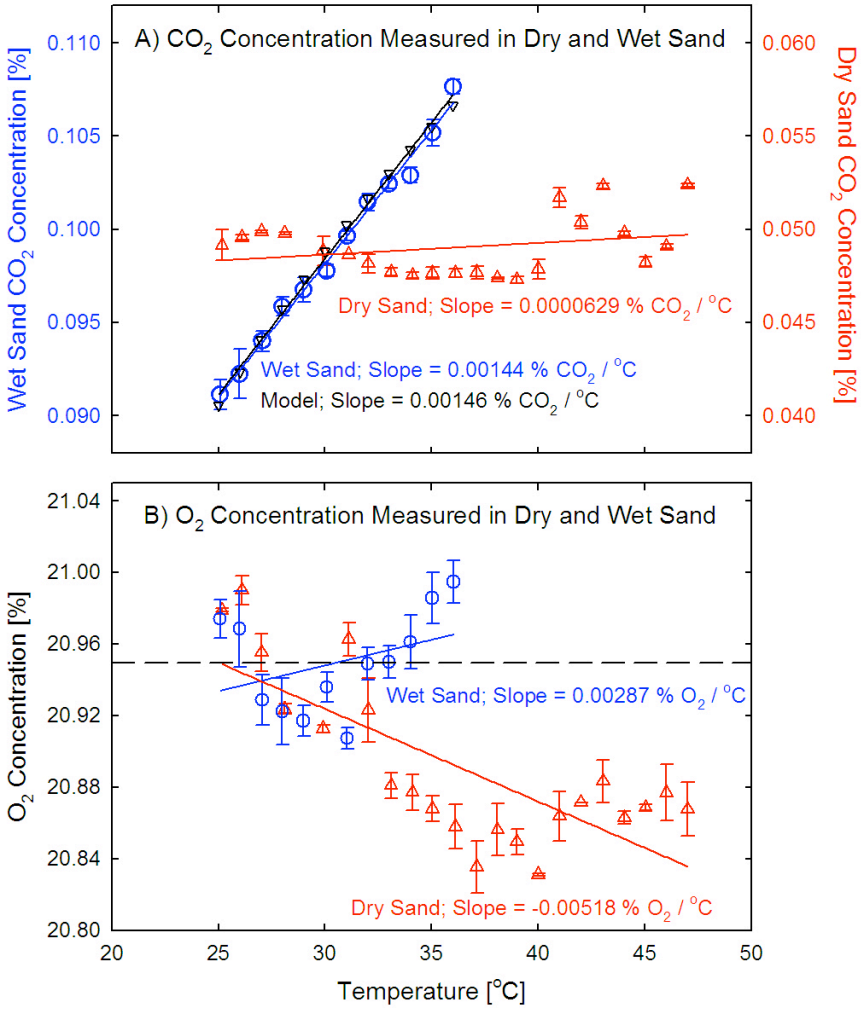

Figure 10: Relative A) CO_2 and B) O_2 concentration [%] measurements in dry and wet sand. The CO_2 concentration in wet sand (circles, corresponds to left hand y-axis) is compared to a model showing how CO_2 solubility affects CO_2 concentration as a function of temperature.